ELSEVIER

PII: S0141-3910(96)00162-0

Polymer Degradation and Stability **55** (1997) 347–365

0141-3910/97/$17.00

Investigation of the degradation and stabilization of EVA-based encapsulant in field-aged solar energy modules

Peter Klemchuk,[a]* Myer Ezrin,[a] Gary Lavigne,[a] William Holley,[b] James Galica[b] & Susan Agro[b]

[a] *Institute of Materials Science, University of Connecticut, Storrs, CT 06269, USA*
[b] *Springborn Laboratories, Inc., One Springborn Center, Enfield, CT 06082, USA*

(Received 17 June 1996; accepted 11 July 1996)

The discoloration of EVA-based encapsulant in some solar photovoltaic modules, most notably a mirror-enhanced module and others recovered from Carrisa Plains, CA, has been investigated in order to understand the causes of the phenomenon and to find solutions to the problem of reduced electrical output. The discoloration has been found to be due to interactions between cross-linking peroxide and some stabilizing additives, and is also likely to be due to oxidation of the encapsulant. No evidence could be found in field-aged, discolored EVA encapsulant for conjugated double bonds, which has been implicated as the cause of discoloration in earlier publications.

Reformulated encapsulant and the use of cerium-oxide-containing glass as the top cover of PV modules have dramatically reduced discoloration. Additional benefit should be derived by excluding oxygen from the modules.

1 INTRODUCTION

The generation of electricity from terrestrial sunlight by means of silicon-based photovoltaic modules (PV) has become an important source of renewable energy. In view of this, the United States Department of Energy, through the National Renewal Energy Laboratory (NREL), is lending support to the fledgling industry by its own work and by financing investigations which promise to contribute to the growth of the industry. Work sponsored by the Department of Energy in the late 1970s and early 1980s at the Jet Propulsion Laboratories (JPL) and the Springborn Laboratories, Inc. led to the development of a cross-linked ethylene vinyl acetate copolymer (EVA) formulation as encapsulant to protect the delicate silicon wafers, the generators of electricity in the modules. EVA-based PV encapsulant is employed extensively by solar module manufacturers worldwide. It has been in commercial use since 1981,[1] and has proven dependable from the standpoint of production, module fabrication and end-use. Recently, some module producers and end-users have reported instances of discoloration, from yellow to brown, of field-aged modules with concomitant loss of electrical generating efficiency.[2,3] Although few in number, these reports have raised serious concerns as to the long-term reliability of EVA-based encapsulants and question the possibility of achieving the desired 30-year lifetimes and target economics.

The 30-year lifetime objective is particularly challenging for an organic encapsulant. It must retain its properties, which protect the silicon solar cells from breaking, while exposed interminably to terrestrial sunlight and elevated temperatures. The task is particularly challenging when the modules are exposed in regions with high solar irradiance to take advantage of the high photon flux.

A literature search and field surveys have revealed that the discoloration was not the bane

* To whom correspondence should be addressed.

of any single manufacturer, but has been experienced in modules made by all major U.S. manufacturers.[3] Also, the search and surveys disclosed that this discoloration problem is not limited to EVA-based encapsulant sheet made by any one supplier. It was apparent from the review that the degree of discoloration appeared to loosely correlate with the degree of average daily direct normal solar radiation, and the module's maximum operating temperature.

Pern and Czanderna of NREL, reported acetic acid generation, unsaturation formation, reduction in ultraviolet absorber (UVA) concentration, and spectroluminescence accompanied the field-exposure of PV modules with cross-linked EVA-based encapsulant.[4] Their findings and information in other publications[5,6] guided our initial approaches to studying the discoloration phenomenon.

The objective of this present study was to generate an understanding of the discoloration, yellowing at first and ultimately browning, of cross-linked EVA which can accompany its use as an encapsulant in silicon-based PV modules, when used in the field to generate electricity from terrestrial sunlight. To this end, field-aged, both mirror-enhanced and non-mirror-enhanced, EVA-encapsulated modules from an affected site in Carrisa Plains, CA, were autopsied. Encapsulant samples were analyzed for vinyl acetate contents, unsaturation, additive concentrations, carbon–oxygen ratios, and metals by thermogravimetric analysis (TGA), Fourier transform infrared analysis (FTIR), resonance-enhanced Raman spectroscopy (Raman), thermal desorption gas chromatography/mass spectrometry (GC/MS), gas chromatography/flame ionization detection (GC/FID), X-ray photoelectron spectroscopy (XPS), and scanning electron microscopy–energy dispersive X-ray spectroscopy (SEM–EDX). The constituents of the EVA-based encapsulant formulation were investigated relative to their discoloration potential on exposure to simulated terrestrial sunlight. This was done with in-house prepared and photo-aged laminate samples. Also examined was the influence of the peroxide cross-linking agent on additive concentrations and discoloration. As a result of the knowledge gained from this work, new encapsulant formulations have been developed in which problematic constituents have been replaced. These new formulations, in conjunction with new cerium-containing glasses, offer the promise of being more likely to achieve the desired 30-year module lifetime than the formulation which has been used.

2 BACKGROUND

Photovoltaic modules are complex constructions. A schematic drawing (Fig. 1) shows a top cover, usually glass, below which are a layer of encapsulant, the silicon cell, a second layer of encapsulant and a bottom protective backing layer. The top cover provides environmental isolation, can attenuate the far UV portion of terrestrial sunlight and contributes rigidity to the fabrication. If glass, the top cover also serves as a non-permeable barrier. The backing layer provides electrical and environmental isolation and a mechanical barrier. Depending on the material of construction, the back cover provides varying degrees of diffusion control. Ideally, it is a barrier to the diffusion of oxygen, but most plastic backing materials, such as Tedlar, are less effective diffusion barriers than glass. The top view of a single solar cell is shown in Fig. 2.

The properties of the encapsulant are critical to the long-term performance of modules. The silicon solar cells are so fragile that an encapsulant is needed to protect them against cracking and breaking. The modulus of elasticity of the encapsulant was concluded to be most sensitive in an investigation of critical life-limiting properties of PV modules.[7] An increase in modulus was seen to cause increased cell stress from thermal and deflection stresses. An encapsulant in which the modulus increased with age, as from oxidation and cross-linking, was expected to lead to cracked cells and to easily cause failure.

During the original work performed by Springborn Laboratories, Inc. under contract to JPL,[8] several alternative materials were investigated as encapsulants for photovoltaic cells. The initial screening criteria for the ideal encapsulation material included the characteristics pre-

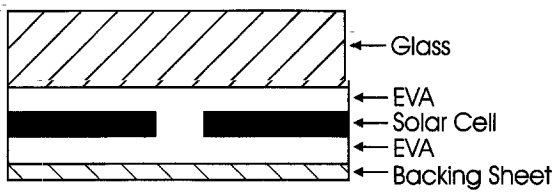

Fig. 1. Schematic cross-section of solar cell.

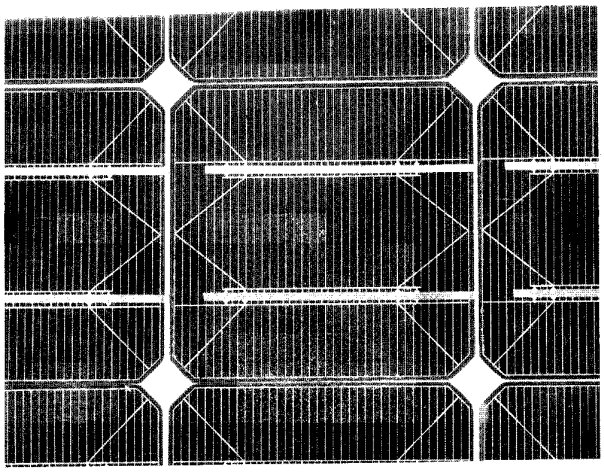

Fig. 2. Photograph of a single solar cell.

sented in Table 1. Vacuum lamination and liquid casting were investigated as fabrication processes for the specific materials in that work. The initial candidate polymers included polyvinyl chloride (PVC) homopolymers and copolymers, polystyrene, polyolefin homopolymers and copolymers, polyesters, polyvinyl alcohol, ionomers, acrylics, polyamides, cellulosics, polyurethanes and silicones, among others. The possible candidates were reduced further based on optical transparency, modulus, processability and cost. The final candidates selected for further development in the JPL program included two types of liquid casting resins, polymerizable butyl acrylate syrups and aliphatic urethanes, and two lamination polymers, ethylene vinyl acetate copolymer (EVA) and ethylene methyl acrylate copolymer (EMA).

The main purpose for the development of liquid systems was to offer module manufacturers the flexibility to pursue fabrication concepts other than vacuum lamination. A final stabilized butyl acrylate system was formulated to produce a transparent low modulus rubber which was found to be suitable as a pottant material. However, major objections to the use of this material were the pungent odor of the monomeric butyl acrylate, use of which requires good ventilation, and the high exotherm which results from its high heat of polymerization during cure.

A two-part aliphatic polyurethane system was also developed with the assistance of Development Associates, Inc., a supplier of liquid urethane systems. The colorless developmental material demonstrated resistance to UV degradation in the laboratory. Inadequacies with this system were caused primarily by poor bond strengths to substrates other than glass and the limited pot life of the mixed two-part system, i.e. 15 min. Primers from the manufacturer for improved bond strengths were available, but this system was not pursued to commercial status during the program.

Of prime choice in the JPL-funded development work were the lamination systems based on Dupont's Elvax 150 EVA resin having a 33% vinyl acetate content and 43 g/10 min melt index (ASTM D 1238). This resin was formulated to be cured in place during module lamination

Table 1. Encapsulant material specifications[8]

1.	Glass transition temperature (T_g)	< -40°C
2.	Total hemispherical light transmission through a 20 ml thick film integrated over the wavelength range from 0.4 to 1.1 μm	>90% of incident
	Hydrolysis	None at 80°C, 100% RH
	Resistance to thermal oxidation	Stable up to 85°C
	Mechanical creep	None at 90°C
	Tensile modulus as measured by initial slope of stress–strain curve	<3000 psi at 25°C
	Fabrication temperature	<170°C for either lamination or liquid pottant systems
	Fabrication pressure for lamination pottants	≤1 atm
	Chemical inertness	No reaction with embedded copper coupons at 90°C
10.	UV absorption degradation	None at wavelength >0.35 μm
11.	Hazing or clouding	None at 80°C, 100% RH
12.	Minimum thickness on either side of solar cells in fabricated modules	6 ml
13.	Odor, human hazards (toxicity)	None
14.	Dielectric strength	Sufficient to electrically isolate the cells and interconnects
	Process compatibility	Compatible with automated cell handling and encapsulation equipment
16.	Cost	As low as possible

and formulated with stabilizers for field exposure. The current commercially available lamination encapsulants sold by Springborn Laboratories, Inc., and others, are based upon this technology. The second lamination formulation was based on ethylene methyl acrylate copolymers from Chevron Chemical Co. This system was not commercialized because satisfactory laboratory and field results were achieved with the EVA-based system as the primary encapsulant material. However, from the laboratory work conducted with the EMA material, it appears that the EMA systems processed similarly to EVA.

The following formulation of the EVA-based encapsulant sheet A9918P, as manufactured by Springborn Laboratories, Inc. for photovoltaic modules, was used extensively in this work. Formulations of other manufacturers of EVA-based encapsulant sheet are presumed to be similar. During lamination for 1 h at 150°C to produce the module, the EVA is cross-linked to 80–90% gel.

Springborn Laboratories' A9918P formulation

Constituent	*Parts*
Ethylene vinyl acetate copolymer, 33% VA (EVA)	100.0
2,5-Dimethyl-2,5-di-*tert*-butylperoxyhexane (peroxide)	1.5
2-Hydroxy-4-octoxybenzophenone (UVA)	0.3
bis(2,2,6,6-Tetramethyl-4-piperidinyl) sebacate (HALS)	0.1
tris(Nonylphenyl)phosphite (phosphite)	0.2
γ-methacryloxypropyl trimethoxy silane	0.25

Several of the field-aged modules examined in this work were obtained from the Carrisa Plains, CA solar photovoltaic power plant, the world's largest.[6,9] The plant came on line in late 1983. It consisted of nine segments with 60° angled mirrors, which reflected sunlight onto the surfaces of the modules to increase the total radiation to a nominal two suns. Each segment was mounted on two-axis trackers to optimize the exposure to the sun on a daily and seasonal basis. A tenth segment, added in 1985, was not mirror-enhanced. Each segment was rated at 633 kW dc, about 58.9 W per module (10 752 modules, 387 072 individual solar cells per segment).

The Carrisa Plains plant was rated originally at 5.2 MW ac. By 1990, the output had fallen to less than 3 MW ac. The degradation was attributed partially to browning of the EVA-based encapsulant. Part of the problem was attributed to the mirror enhancement which caused high operating temperatures. Moreover, the concentrators were apparently used on modules which had been designed for one-sun use.

3 EXPERIMENTAL

3.1 Materials

The materials used in laboratory-prepared samples were commercial products obtained from their manufacturers and used without further treatment. EVA resin was Dupont's Elvax 150, containing nominally 400 ppm butylated hydroxytoluene (BHT). 2,5-Dimethyl-2,5-di-*tert*-butylperoxyhexane was Lupersol 101, 2-hydroxy-4-octoxybenzophenone was Cyasorb UV 531, bis-(2,2,6,6-tetramethyl-4-piperidinyl) sebacate was Tinuvin 770 and tris(nonylphenyl)phosphite was Naugard P. EVA formulation A9918P was Springborn's 'standard-cure' EVA, the composition of which is shown above. EVA formulation 15295P was Springborn's 'fast-cure' EVA, the composition of which was identical to A9918P, except that the peroxy cross-linker was *tert*-butyl 2-ethylhexyl percarbonate, Lupersol TBEC.

The field-aged modules studied in this work were recovered from service at the Carrisa Plains, CA power plant and other installations. Identities of specific panels are summarized in Table 2. The backing plastic on the modules was a white-pigmented Tedlar/polyester/Tedlar laminate.

Coupon-sized glass/glass laminates, measuring 6.86×6.99 cm, with approximately 0.046 cm inner layers of formulated EVA were used for comparative laboratory-accelerated photo-aging studies. Edges of uncured laminates were sealed with an epoxy adhesive; edges of cured laminates were not sealed. Glass/glass laminates were used in order to facilitate visual, colorimetric and spectrographic measurements. All were prepared by vacuum lamination on laboratory-scale equipment using the commercial time/temperature/vacuum schedule, 1 h at 150°C, recommended for 'standard-cure' EVA. During cure, a data logger and multiple thermocouples were used to verify the temperature profile of all samples cured in the laminator. Gel contents of the cross-linked

Table 2. Identities of solar photovoltaic modules

Module	Source of EVA	Discoloration	Mirror enhanced	Years in service
#1[a]	Richmond (Siemens)	Slight	No	8
#2[a]	Richmond (Siemens)	Moderate	No	8
#3[a]	Richmond (Siemens)	Severe	Yes	10
#A1	Springborn (Solarex)	None	No	est. 2–3
#A2	Springborn (Solarex)	Slight	No	est. 2–3

[a] Carrisa Plains.

A9918P formulation in commercial modules are typically 80–90%.

Given our interest in achieving maximum cell efficiency, including conversion of UV-B photons to electricity, a low iron glass superstrate was selected for the laminates. It should be noted that UV-B transmission (i.e. 285–330 nm) is the wavelength region suspected of being most responsible for EVA discoloration/degradation. This decision was further reinforced by the fact that low iron glass was the superstrate most commonly used in those field modules which had shown discoloration. Specific low iron glasses tested were AFG's Solite (samples from the mid-1980s), PPG's Starphire, AFG's Solatex II (containing less than 4% cerium oxide by weight) and PPG's Solarphire (also containing cerium oxide).

3.2 Analytical methods

3.2.1 Preparation of specimens for analysis

Specimens from field-aged modules were obtained by cutting through the back plastic cover and peeling the encapsulant away from the silicon and the glass top. For some analyses, to obtain information about more discolored areas (nearest the top glass cover) and less discolored areas (under the silicon cells, between cells and along edges), EVA was cut with a small sharp knife from a top relatively discolored section and a bottom largely undiscolored portion.

EVA, laminated between glass plates and laboratory-aged, was sampled using a hand-held modified bandsaw blade. The teeth of the thin bandsaw blade were ground so as not to protrude to the side. Thus, glass was not abraded and mixed with the sample. The resultant sample was in the form of small particles.

Samples of uncured EVA sheet were wrapped in aluminum foil and stored in a refrigerator to minimize peroxide decomposition. Particles sawed from cured and unaged laminates were analyzed immediately after being sawed.

3.2.2 Vinyl acetate content by TGA (thermogravimetric analysis)[10]

The vinyl acetate content of EVA samples was determined from the weight loss by TGA in nitrogen. Acetic acid is quantitatively and rapidly evolved from EVA starting at about 300°C (Fig. 3). Sample weight is corrected for ash content, if any (residue at end of run). TGA instruments from Dupont and TA Instruments Co. were used. The programmed heating rate was 5°C/min in early work with the Dupont TGA. In later work, with the TA Instruments high resolution TGA, in which the rate of rise is reduced to practically zero automatically when weight loss occurs, the programmed heating rate was 20°C/min.

3.2.3 Determination of additives content by thermal desorption gas chromatography/mass spectroscopy (GC/MS)

The procedure and the apparatus used at UConn-IMS have been described.[11] Samples were heated in the injection port of a GC to transfer volatile compounds into a GC column where they were separated during a temperature program. Mass spectral peaks identified compounds and peak areas were used to quantita-

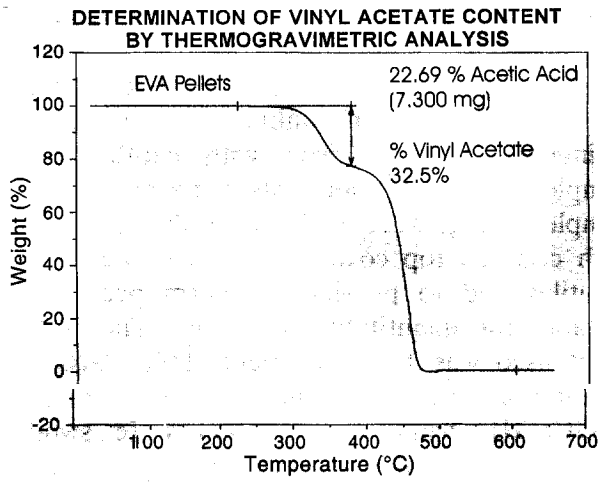

Fig. 3. Determination of vinyl acetate content of EVA by TGA.

tively determine BHT (present in EVA resin as received from Dupont), UVA and HALS. The phosphite could not be determined by this method. The MS method is so sensitive that samples were limited to ca. 0.2 mg for good quantitative analysis. The very small sample size led to the use of GC/FID (flame ionization detector) (see below) with which a sample size of ca. 2 mg could be used, thus assuring a more representative sample. Duplicate or triplicate analyses were conducted for all analyses with satisfactory replication.

BHT, UVA and HALS were all determined quantitatively first by the GC/MS method. The latter two were then determined more accurately by GC/FID. The values for BHT, however, are based on GC/MS.

GC column and conditions were as follows: Instrument—Hewlett/Packard 5890IIGC/5971A mass selective detector; column —SGE BPX-5, 25 m × 0.2 mm ID, 1.0 μm film thickness; sample size—ca. 0.2 mg; thermal desorption—2′/350°C; oven program—35–350° at 15°C/min; mass spectrometer—selected ion data collection using masses specific for UVA, HALS and BHT.

3.2.4 Determination of additives content by thermal desorption GC/FID (flame ionization detector)

The GC column and conditions for FID detection were as follows: column—SGE BPX-5, 25 m × 0.2 mm ID, 1.0 μm film thickness; sample size—ca. 2 mg; thermal desorption—2′/350°C; oven program—40–300°C at 15°/min.

3.2.5 Peroxide content by DSC and by GC/FID

DSC: In this method the relative peroxide content was measured by the exotherm accompanying the decomposition of peroxide and cross-linking of EVA. The relative percent peroxide content of unknown samples was estimated by comparison with exotherms of samples with known amounts of peroxide. Small samples (2 mg) were enclosed in aluminum pans with crimped top covers to prevent the loss of volatiles and to provide exotherm peak areas suitable for quantitative purposes. The instrument used was TA Instruments DSC 2920; the heating rate was 20°C/min.

GC/FID: Samples (0.2–2.0 g) were swollen overnight in 100 ml methylene chloride to obtain quantitative removal of peroxide; injections of aliquots were made into the GC. The GC column and conditions were as follows: column—100% methyl silicone, 15 m × 0.53 mm ID, 1.5 μm film thickness, 15 psi; oven program—40–160°C at 20°/min; injection port—100°C; temperatures were kept below the decomposition temperature of the peroxide.

3.2.6 Infrared spectroscopy

Infrared spectroscopy was used to study double bonds, oxidation effects, acetate contents, etc. The acetate group contributed infrared absorption bands at 1737 (carbonyl) and 1242 cm^{-1} (ether). The total carbon–hydrogen content was reflected in the carbon–hydrogen region at 2921 and 2820 cm^{-1}. Thin specimens of the same samples as in the XPS section below were used to obtain spectra with a Spectra-Tech Micro-IR together with a Nicolet 60SX Fourier transform infrared spectrometer (FTIR). Ratios of the 1737 cm^{-1}/2820 cm^{-1} and 1242 cm^{-1}/2820 cm^{-1} absorbance bands provided relative measures of vinyl acetate contents. The absorbance of the methyl group at 1371 cm^{-1}, relative to 2820 cm^{-1} provided another, less reliable, relative measure of vinyl acetate content.

3.2.7 X-ray photoelectron spectroscopy for vinyl acetate content and carbon–oxygen ratios

XPS was performed with a Perkin-Elmer 5300 series XPS equipped with a monochromatic Al Kα X-ray source, hemispherical analyzer and position sensitive detector. Samples were cleaned with an isopropanol wipe and a hexane wipe before insertion into the prechamber for degassing. Data were collected at 15 kV and 600 W. After an initial survey scan, several acquisitions were made at a pass energy of 35 eV, and then a high resolution scan at 8.6 eV. All of the data for a given sample were acquired within 30 min, well below the time it takes for the monochromatic X-ray source to significantly damage a sample (approx. 6 h).[12] Multiple acquisitions on the same sample were averaged and the degree of precision was calculated.

The samples analyzed were removed from a highly discolored field-aged module, Module #3 from Carrisa Plains, CA. Only the top side of the EVA-based encapsulant in contact with glass was discolored. The bottom side, in contact with the cells, was practically non-discolored. XPS was performed on the top and bottom sides, on colorless diamond-shaped regions at the juncture of four cells and on unaged EVA.

3.2.8 Resonance-enhanced laser Raman spectroscopy for olefinic unsaturation

Laser output at the sample was 1–2 MW and beam diameter was 10 μm. The laser beam was 514.5 nm Ar^+ ion (as a result of halving the frequency of the laser beam, the actual wavelength applied to the sample was 257 nm). Samples were moved on a microscope slide in the focal plane of a Cassegrain objective at the rate of approximately 10 oscillations per second. The spectra were collected over a period of 2.5 min using an EG + G diode array system. Dispersion was due to a 2400 g/nm grating optimized at 250 nm. Slits were approximately 200 μm giving rise to an approximate 8–10 cm^{-1} spectral slit.

The samples analyzed were three PVC samples and three EVA-based encapsulant samples. The same PVC (heated for 20 min at 180°C) as below in Section 3.3.1, was run in addition to PVC heated for 70 min at 180°C and for only 2 min at 180°C (pressed only). Both the 20 and 70 min samples were discolored, though the latter was more highly discolored than the 20 min sample. The PVC samples provided a control for conjugated C=C unsaturation, because PVC is known to discolor due to long conjugated double bonds formed by dehydrohalogenation (loss of HCl) on thermal aging. The EVA-based encapsulant samples were: (1) cured and unaged production sheet from Springborn Laboratories; (2) cured as a laboratory laminate with the same construction as large modules, but not aged; and (3) field-aged Carrisa Plains Module #3 as above, top and bottom surfaces.

3.2.9 Analyses for metals using scanning electron microscopy–energy dispersive X-ray spectroscopy (SEM–EDX)

The instrument used was an Amray 1000A SEM with a Kevex Delta 4 EDX system. The accelerating voltage was 20 kV. Samples were carbon coated.

3.3 Other methods

3.3.1 Reaction of peracetic acid with discolored PVC and EVA-based encapsulant

PVC sample: A sheet of film 0.127 cm thick was prepared by compression molding virgin PVC powder without a stabilizer at 180°C for 2 min. The resultant PVC film was heated at 180°C in an oven for 20 min. The thermally degraded PVC sample was colored very dark brown, almost black.

EVA-based encapsulant: A sample of encapsulant, which had been in contact with the glass top, was cut from discolored Carrisa Plains Module #3, the solar module with the darkest color.

Each sample was placed in a closed flask with 25 ml of chloroform and allowed to swell for 24 h with adsorbed chloroform. Five millilitres of 32% by weight peracetic acid in acetic acid (Aldrich 26,933-6) was added to each flask. The flasks were swirled and allowed to stand for an additional 24 h.

3.3.2 Accelerated photo-aging

Indoor exposures for simulated photo-aging were carried out in an Atlas Ci35A Xenon-arc Weather-Ometer (XAW) with quartz/borosilicate glass filters. The nominal lower end UV cut-off was 285 nm. Duplicate samples of each formulation were exposed. During testing, all coupon laminates were exposed to an irradiance of 0.55 $W/m^2/nm$ at 340 nm, roughly the equivalent of two suns,[13] at a black panel temperature of 100°C, until significant degradation/discoloration had occurred. The samples were rotated from top to bottom and between racks on a weekly basis so as to normalize any minor temperature/irradiance differences.

Exposures for accelerated weathering were carried out at DSET Laboratories, Inc. in Arizona according to ASTM standard D 4364. The machine used was an equatorial mount with mirrors for acceleration (EMMA).

3.3.3 Color measurements

All samples were monitored for any color development/changes during exposure. Non-destructive tests which were performed included yellowness index per ASTM D-1925 and percent light transmission (%T) between 250 and 900 nm via UV–visible spectroscopy (UV–VIS).

4 EXPERIMENTAL RESULTS

4.1 Vinyl acetate contents by TGA

Analyses were performed on EVA-based encapsulant samples representing a wide range of exposure history, including uncured and unaged

EVA. In all instances, from virgin EVA resin to the most highly degraded encapsulant, the thin darkest layer of Module #3, the percent vinyl acetate was virtually within the experimental error of the 33% value for unaged EVA (Table 3). The range of values was from 32.6% to 35.5%. There appears to be a statistically unconfirmed trend in the data for higher values in the more degraded samples, suggesting that the more degraded samples experienced less degradation of polyvinyl acetate segments than polyethylene segments.

Even though acetic acid was detected by GC/MS at levels of 0.10–0.15% in field-exposed panels immediately on opening, the amount present did not reflect a significant reduction in vinyl acetate contents of the encapsulant.

Everything considered, there appears to be little double bond formation from photolysis of vinyl acetate. If there is little basis for double bond formation at any level, there is even less reason to expect conjugated double bond sequences of eight or more as required to develop color in the copolymer.

4.2 Stabilizer contents of encapsulant from field-aged modules by GC/MS

As expected, in view of potential consumption during cross-linking/lamination and in view of photo-instability, the BHT contents of all field-aged samples were markedly lower than the nominal 400 ppm added in production (Table 4). The UVA contents of the samples from Carrisa Plains showed low levels above the silicon cells and higher levels in the clear areas between cells. The clear areas are in contact with the encapsulant below the silicon cells and can be replenished from that source. The less weathered, less degraded panels, A1 and A2, contained higher levels of UVA. The HALS showed lesser reductions in concentration than the UVA.

4.3 Influence of peroxide on color and stabilizer concentrations of laboratory-aged samples

Laboratory-prepared samples with glass on both sides of the EVA-based encapsulant, which were photo-aged in the XAW, showed that peroxide caused marked lowering of UVA and HALS concentrations (Table 5). The UVA concentration was practically unchanged after 10 weeks exposure, in an EVA formulation without peroxide, but dropped by 40% after 12 weeks exposure when peroxide at the usual level, 1.5 pph, had been included in the formulation. Similarly, the HALS concentration dropped by 61% when the peroxide was included. Clearly, during lamination, the peroxide interacted with the UVA and the HALS which reduced their concentrations and, in the case of the UVA, caused color formation. EVA with HALS and no UVA did not discolor in the presence or absence of peroxide.

Laboratory-aged samples of virgin Elvax 150, without stabilizing additives, did not develop significant amounts of color after aging for 15 weeks in an XAW (Table 6). Under the same conditions, cross-linked EVA containing all the additives of the standard formulation A9918P, discolored significantly. The samples with all the additives except the peroxide, and those with all but the UVA discolored only moderately. The data in Table 6 indicate that much of the discoloration problem is likely to be due to interactions between the peroxide and two stabilizing additives, the UVA and the phosphite.

Table 3. Analysis of EVA encapsulants

% vinyl acetate content by TGA			
Standard-cure A9918P		Fast-cure 15295P	
Description	%VA[a,b]	Description	%VA[a,b]
Uncured sheet	33.2	Uncured sheet	32.4
Cured, unaged	34.9	Cured, unaged	32.8
Weather-ometer aged, 12 weeks (light yellow)	33.5	Weather-ometer aged, 25 weeks (yellow)	32.1/32.6
Carrisa modules (brown)	33.9–35.5	Weather-ometer aged, 34 weeks (amber)	33.0/33.6

[a] Corrected for ash residue.
[b] 32.6% for Elvax 150 as received.

Table 4. Analytical results for BHT, UVA and HALS by GC/MS[a]

Sample ID	BHT (ppm)		UVA (ppm)		HALS[b]	
	Over solar cell	Between cells	Over solar cell	Between cells	Over solar cell	Between cells
Unaged EVA cured sheet	216		3650		13.6	
Unaged laboratory laminate	259		2650		11.0	
Module #1	7.7	13.9	100[c]	1750	4.4	3.5
Module #2	8.0	12.6	100[c]	1400	3.7	3.2
Module #3	10.7	15.1	100[c]	1500	4.4	4.5
Module A1	5.8	10.2	1500	3550	11.4	1.8
Module A2	15.6	24.3	1750	4200	9.0	12.2

[a] Average of three or more determinations, estimated values.
[b] Peak measured in total ions, uncalibrated, $\times 10^{-8}$.
[c] Estimate 50–100 ppm.

The HALS appears to be a less likely contributor to discoloration. This experimental evidence from the XAW exposures suggests that discoloration of the EVA-based encapsulant might be due, at least in part, to transformation of additives caused by photolysis in the presence of peroxide.

These results are in disagreement with the hypothesis that the discoloration is due mainly to long sequences of conjugated double bonds.

4.4 Peroxide concentrations in stored and laboratory-aged EVA samples

As shown by data in Table 7 obtained by GC/FID, about 1/4 of the peroxide charged to the A9918P formulation persisted through the lamination/cross-linking procedure. Exposure for more than 2 weeks in the XAW was required subsequently to destroy the peroxide completely. This suggests that reactions between peroxide and stabilizing additives can take place from the time when the formulation is prepared through to the time when the peroxide is consumed on exposure to light. Chromophore precursors and chromophores might be generated all the time that peroxide is present in the formulation. The lamination step, because of the relatively high temperatures and presence of free radical intermediates, and the period of light exposure with peroxide present are thought to be significant for the discoloration problem.

Analyses were carried out also by DSC for the peroxide in retained samples of production lots of A9918P stored for up to 1 year at ambient conditions. Data in the following table for the analysis of peroxide by DSC show only small, if any, losses on storage at Springborn of the production lots for up to 1 year. The DSC method was satisfactory for uncured encapsulant using samples of uniform size which had been punched out from the sheet. Reproducibility was less satisfactory for cured laboratory-aged samples using odd-shaped specimens.

Table 5. Effect of peroxide and XAW-aging on color and stabilizer concentrations by GC/FID

Peroxide	XAW	YI	UVA (area/mg $\times 10^{-4}$)		HALS (area/mg $\times 10^{-3}$)	
			Conc.	Change	Conc.	Change
None	None	0.5	5.30		17.1	
None	10 weeks	5.4	5.29	0%	16.2	−5%
1.5%	None	1.7	5.39	—	None	
1.5%	12 weeks	14	3.22	−40%		
1.5%	None	0.5	None		9.18	
1.5%	12 weeks	1.0			3.56	−61%
None	None	−0.3	None		14.9	—
None	6 weeks	−0.8			15.6	None
None	None	−0.2	5.99		None	
None	11 weeks	−0.9	6.09	None	—	

Table 6. Yellowness index after XAW-exposure of A9918P EVA-based glass/glass laminates with additives removed or added

Formulation	YI after exposure in XAW		
	5 weeks	10 weeks	15 weeks
A9918P	7.7	19.2	43.5
No additives	1.2	1.2	2.0
No peroxide	1.9	6.3	
Only peroxide	0.5	1.1	0.9
No UVA	6.6	6.0	6.8
Only UVA	0.3		
Only peroxide and UVA	6.8	11.5	19.4
No HALS	7.7	16.8	
Only HALS	0.2		
No phosphite	6.4	11.0	17.7
Only phosphite	1.7	5.3	9.3

Concentrations of peroxide in production lots of A9918P (by DSC)

Production date	*Relative peroxide concentration*
9/7/94	10.5 J/g
8/94	10.5 J/g
3/94	11.3 J/g
9/93	9.8 J/g

4.5 Resonance-enhanced laser Raman spectroscopy

Raman spectroscopy supplements infrared spectroscopy in that weak bands in the IR are generally strong in the Raman. Thus, while C=C unsaturation, postulated to be the cause of discoloration, does not absorb strongly enough in the IR to be reliable as an indicator of the presence of unsaturation, Raman does provide strong reliable bands. However, Raman suffers from the effect of fluorescence on spectra, a condition which is true for discolored EVA-based encapsulant. Resonance-enhanced laser Raman spectroscopy reduced this effect sufficiently to permit useful spectra to be obtained. The spectra are largely of the surface analyzed, since the laser energy that is measured is scattered from the surface.

Table 7. Concentrations of peroxide in Formulation A9918P at various stages by GC/FID

Stage	Conc. (%)
Formulation charge to production lot	1.5
Extruded sheet, production lot	1.15
Laboratory-prepared glass/EVA/glass laminate	0.37
XAW-exposed laminate, 2 weeks	0.03
XAW-exposed laminate, 12 weeks	0.00

The ability of Raman to detect C=C double bonds, via absorption bands at 1650 cm^{-1}, as they relate to discoloration, was demonstrated with PVC. The slightly discolored PVC film sample, which had been prepared by compression molding at 180°C for 2 min, exhibited a relative intensity of approximately 0.6 for the 1650 cm^{-1}/1450 cm^{-1} bands. The latter is a reference band for PVC. A dark colored sample of PVC film, which had been heated for 70 min at 180°C, exhibited a relative intensity of approximately 9.0 for the same two bands, easily an order of magnitude increase. Clearly, Raman is very sensitive to C=C double bonds.

Resonance-enhanced Raman spectra were obtained for unaged EVA-based encapsulant and for the discolored top surface of Carrisa Plains Module #3. While fluorescence had an adverse effect on the spectrum of discolored EVA-based encapsulant, the band at 1620 cm^{-1} was very clear, as it was for the unaged sample. There was not an absorption band at 1650 cm^{-1} corresponding to induced unsaturation. The Raman results provide no evidence for unsaturation in the dark EVA-based encapsulant. The spectrum of the lightly discolored bottom side of Module #3 was the same as that of the discolored top side. If there were significant unsaturation in the dark top layer of EVA-based encapsulant in Module #3, it should have been seen at 1650 cm^{-1}, the characteristic wavelength for C=C as shown by PVC, and the spectrum should have been different from that of the bottom surface.

When the 257 nm beam was allowed to stay at one point on the sample for more than about 2 min, the 1650 cm^{-1} band for C=C was increased in the PVC samples and formed in the EVA-based encapsulant samples. Apparently, both PVC and EVA are capable of generating a double bond by eliminating an acid group, i.e. HCl for PVC and acetic acid for EVA, under the influence of an intense UV band at 257 nm. In actual solar modules the glass top shields the encapsulant from radiation of that wavelength. The fortuitous case of the 1650 cm^{-1} band being formed for EVA-based encapsulant demonstrates that EVA will deacetylate and form double bonds under certain conditions (257 nm), but it clearly did not happen in end use due to protection from the glass, and, more importantly,

because the spectrum of terrestrial sunlight ends at about 290 nm.

4.6 X-ray photoelectron spectroscopy

One of the reasons for selecting XPS is that it measures elemental composition and structure at a surface depth of a little more than 100 Å (0.01 μm).[14] Discoloration of EVA-based encapsulant began at a very thin layer at the interface directly under the glass cover. XPS offered the possibility of identifying the composition in the most discolored part of the EVA-based encapsulant. If vinyl acetate ($-CH_2CH(OCOCH_3)-$) is deacetylated to ($-CH{=}CH-$), two oxygen atoms are removed from the polymer, which should significantly reduce the oxygen content and raise the carbon/oxygen ratio. XPS can also determine the number of carbon atoms in the polymer which are specific to the acetate, i.e. the C* in $\{-CH_2CH[O(O{=}C^*)CH_3]-\}$.

Figure 4 is the XPS spectrum for the highly discolored, embrittled, top surface of the EVA-based encapsulant from Carrisa Plains Module #3, showing resolution of five peaks. Peaks 1 and 2 provide a measure of the methylene carbon atoms in the backbone and the methyl group of the acetate group, respectively. They are combined for interpretation of the data because they occurred within the same peak, and it proved difficult to calculate their amounts separately and accurately. Peak 3 arose from methine carbons adjacent to oxygen. Peak 5, from the carbon of the ester carbonyl, is unique

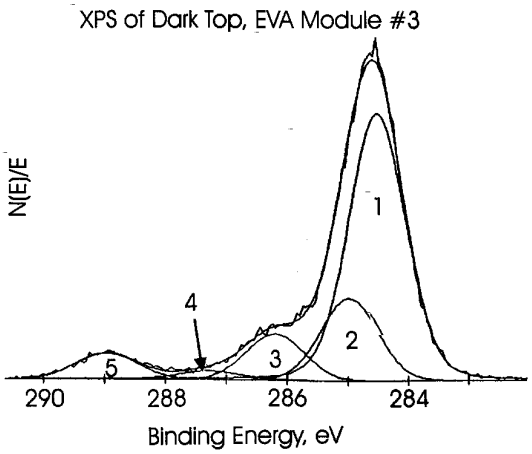

Fig. 4. XPS spectrum of discolored encapsulant from top of field-aged Module #3.

for the acetate group, and peak 4 measured keto-carbonyl, which resulted apparently from oxidation of methylene groups, discussed further below. Peak 4 is absent in the spectrum of unaged EVA-based encapsulant and is smaller for the undiscolored bottom surface of EVA-based encapsulant of Module #3 in contact with the silicon wafer.

Table 8 gives the atomic percent of carbon atoms in methyl, methylene, methine, keto and acetate carbonyl groups for four EVA-based encapsulant samples: laboratory-cross-linked but unaged laminate; a segment of the Carrisa Plains Module #3 in contact with and above the silicon wafer; the top, highly discolored surface against glass of that module; and a clear, diamond-shaped area where four silicon cells meet (Fig. 2). Also included are calculated values for EVA with 33 wt% vinyl acetate. The information in Table 8 clearly shows a progression of increased oxidation from the starting EVA resin and laboratory-prepared laminate as starting references, through the less discolored bottom segment of the field-aged module to the highly discolored top surface. The oxidation is manifested by reduction in methylene and methyl carbon, increase in methine carbon adjacent to oxygen (Peak 3), formation of keto-carbonyl (Peak 4) and increase in ester-carbonyl (Peak 5). The clear, diamond-shaped areas between cells also showed oxidation, including possibly carboxylic acids and esters but not ketones.

Data in Table 9 for the same five materials clearly confirm extensive oxidation in the field-aged module. The oxygen at.% had increased from a little over 11% for the two reference samples to over 17% for the most discolored sample, an increase of over 50%. The carbon and oxygen at.% values for the five materials and the carbon–oxygen ratios are in agreement.

These results strongly indicate that the module construction for the Carrisa Plains, CA installation permitted considerable photo-oxidation of the encapsulant. Presumably, oxygen migrated into the back of the modules through a permeable plastic backing and from the back to the front through the clear areas. Photo-oxidation caused extensive degradation of the top surface of the EVA-based encapsulant. In removing specimens for various analyses it was apparent that the polymer had lost its desirable properties and had become brittle and friable.

Table 8. X-ray photoelectron spectroscopy of EVA samples, compositional analysis

Peak No.	Shift	Peak ID	Atom % C				
			Virgin EVA	Unaged laboratory laminate	Module #3 above silicon	Module #3 below glass	Module #3 undiscolored area at cell corners[a]
1 and 2	0 (#1) 0.7 (#2)	$-C^*H_2-$ $^*CH_3COOCH$	87.9[b]	87.4	83.8	80.9	83.0
3	1.7	CH_3COOC^*H	6.1[b]	7.1	8.9	10.1	9.0
4	3.06	Keto C*=O	—	—	1.8	2.6	
4a	2.49[c]	Uncertain					1.0
5	4.3	CH_3C^*OOCH-	6.1[b]	5.3	5.6	6.4	7.0
		Total	100.1	99.8	100.1	100.0	100.0

* Carbon atom of relevance.
[a] Top side next to glass.
[b] Calculated for 33 wt% VA EVA.
[c] Assignment uncertain; found in undiscolored area at cell corners only; not found in other samples.

In light of the oxidation result, it was not possible to determine unequivocally, from the XPS results, whether the acetate content had decreased as a result of field-aging but indications are that there probably was not much change. Moreover, the TGA data show no reduction in acetate content. In fact, TGA shows a slight increase in acetate content of aged samples, which is likely to be a consequence of the hydrocarbon segments of the EVA being degraded by extensive oxidation.

It is now known for the first time that oxidation of EVA-based encapsulant had occurred in the Carrisa Plains modules. The XPS results indicate that the usual oxidation products were likely to have been formed.

4.7 Peracetic acid treatment of discolored EVA-based encapsulant and PVC

Discolored, partially dehydrochlorinated PVC has been found to be capable of being markedly decolorized by reaction with dienophiles, maleic anhydride and diethyl maleate among others, and hydroxylating agents such as performic acid.[15] These agents react with double bonds and disrupt the conjugation which is responsible for color.

Discolored PVC, aged for 20 min at 180°C, lost all color when treated with peracetic acid, while the discolored field-aged EVA-based encapsulant from Module #3 was unchanged. Results confirm that the reagent and experimental conditions were capable of reacting with double bonds, thus removing the color of the degraded PVC. Failure of the EVA-based encapsulant color to change indicates that its discoloration is not due to long sequences of C=C unsaturation.

4.8 Metal analysis by SEM–EDX

Elemental analysis, in particular for metals, was performed on Carrisa Plains Module #2 by SEM–EDX to determine if material from the conductors on the top of the silicon had ionized

Table 9. X-ray photoelectron spectroscopy of EVA samples, atomic carbon–oxygen ratios

	Sample				
	Virgin EVA	Unaged laboratory laminate	Module #3 above silicon	Module #3 below glass	Module #3 undiscolored area at cell corners[a]
Avg. at.% C	88.9[b]	88.6 ± 0.1	84.6 ± 0.5	82.5 ± 0.2	86.7 ± 0.5
Avg. at.% O	11.1[b]	11.4 ± 0.1	15.4 ± 0.5	17.5 ± 0.2	13.3 ± 0.5
Avg. C–O atomic ratio	8.01[b]	7.77	5.49	4.71	6.52

[a] Top side next to glass.
[b] Calculated for 33 wt% VA EVA.

and migrated into the encapsulant, possibly contributing to discoloration. This was done for the dark top area and for undiscolored encapsulant in the regions between cells. The dark top area showed only silicon, as SiO_2, apparently from glass and/or degraded silane coupling agent, in addition to the carbon and oxygen of the polymer. Copper and silver, which might have come from conductors, were not detected.

4.9 Optical photomicrography

Optical microscopy has shown that the dark portion of discolored EVA-based encapsulant is limited to a relatively thin top section of the encapsulants. It was darkest at the very top of the encapsulant tapering to a lighter color below. For Carrisa Plains Module #3, which was more severely degraded than the other recovered modules, the encapsulant was dark brown at the top, next to the glass, and light brown below. The dark encapsulant top layer was thin, occupying less than 1/10 of the full thickness, i.e. less than 0.05 mm.

4.10 Infrared spectroscopy

Transmission micro-IR spectra of four EVA materials were obtained: (1) cured, unaged, laboratory-made small laminate with silicon and plastic backing, similar construction to the field-aged modules #1–3; (2) Carrisa Plains Module #3, thin cut from dark EVA top in contact with glass; (3) thin cut of the bottom surface of (2) in contact with silicon; and (4) top slice of the clear undiscolored area at the corners of the cells. The thicknesses of the cut samples used for IR were estimated at ca. 0.03 mm, from an overall thickness of about 0.5 mm. Duplicate spectra were obtained with different specimens on each of 2 days, for a total of four spectra of each material. Absorbance ratios were calculated as follows:

$1371\,cm^{-1}/2850\,cm^{-1}$—acetate CH_3/overall CH
$1737\,cm^{-1}/2850\,cm^{-1}$—ester C=O carbonyl/overall CH
$1242\,cm^{-1}/2850\,cm^{-1}$—ester ether C–O–C/overall CH

Figure 5 shows a typical spectrum for EVA of the unaged laboratory-made laminate. The band

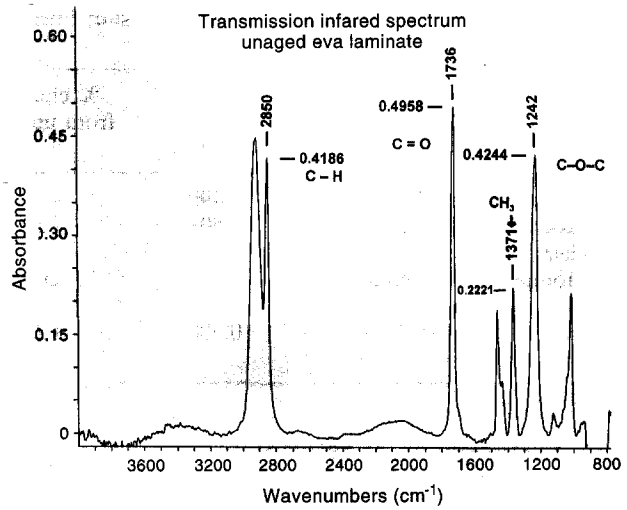

Fig. 5. Infrared spectrum of unaged EVA laminate.

at $2850\,cm^{-1}$ was chosen as the measure of CH instead of the one at $2921\,cm^{-1}$ because it is narrower and less likely to be overloaded. Table 10 gives the average absorbance ratios for the four spectra of each sample.

The most important comparison, which is directly relevant to discoloration of EVA in service, is between (1), unaged, and (2), the dark top of Module #3. For all three parts of the acetate group (CH_3, C=O, C–O–C), the difference between aged and unaged was well within the experimental error.

The $1242\,cm^{-1}$ band is probably the most reliable measure of relative acetate content. The carbonyl at $1737\,cm^{-1}$ might be affected by oxidation of ethylene units, as indicated by XPS. The values for (3) (the bottom of the EVA) might be affected by the difficulty of completely removing the silicon. The values for (4) (the undiscolored area between cells) might have been affected by its greater exposure to oxygen, which migrated through the rear backing sheet, than the EVA above silicon. In any case, IR indicates no measurable difference in vinyl acetate content, for all practical purposes, between unaged EVA and the most highly discolored material analyzed (#3 module, dark top).

The infrared spectra of clear, diamond-shaped encapsulant segments at the corners of silicon cells differed from those of the unaged and aged areas over silicon encapsulant by the presence of a distinct hydroxyl band at approximately $3500\,cm^{-1}$. Light-colored areas over cracks also showed the same band (Fig. 6).

Table 10. Absorbance band ratios by transmission infrared spectroscopy. Unaged EVA laboratory laminate and field-aged Module #3

	1371/2850 methyl CH_3/CH	% change from unaged	1737/2850 carbonyl C=O/CH	% change from unaged	1242/2850 ether C-O-C/CH	% change from unaged
(1) unaged	0.490		1.300		1.080	
(2) Module #3 dark top under glass	0.503	+2.7	1.303	+0.2	1.081	+0.1
(3) Module #3 bottom next to silicon	0.588	+20	1.235	−5.0	1.085	+0.5
(4) clear undiscolored area between cells	0.500	+2.0	1.394	+7.2	1.068	−1.1

4.11 Performance of reformulated EVA-based encapsulants

Four new, proprietary, EVA-based encapsulants, evaluated in laboratory-prepared glass/encapsulant/glass laminates, did not develop any discernible color over 30 weeks of exposure in the XAW (Fig. 7). In the same study, controls with the standard cure A9918P formulation and the fast cure 15295P formulation exhibited yellowness index (YI) increases of 72 and 64, respectively.

4.12 Performance with cerium-oxide-containing glasses

One year of accelerated outdoor EMMA exposure (52 464 MJ/m^2 total irradiance) in Phoenix, AZ resulted in virtually no color development in samples with cerium-oxide-containing superstrate glasses (Solatex II in Fig. 8), whereas the standard cure encapsulant with standard superstrate glass, Solite, had a YI of 29 in a parallel exposure.

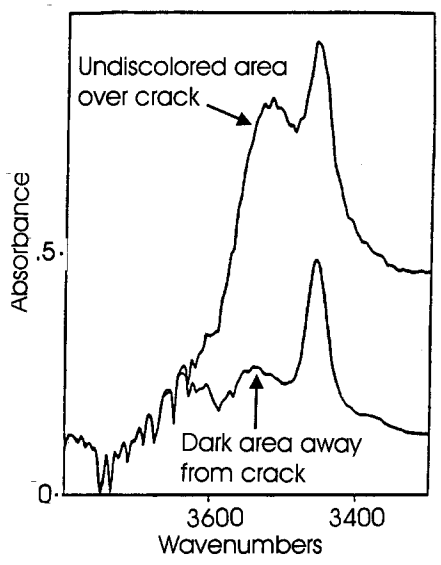

Fig. 6. Infrared spectrum of hydroxyl region of undiscolored area over a crack.

5 DISCUSSION

5.1 Conjugated unsaturation and discoloration of photolyzed EVA

Pern and Czanderna[4] reported the weathering of EVA-based encapsulants in modules increased gel content, decreased UVA concentration and produced acetic acid, other volatile organics and double bonds. They proposed that acetic acid and double bonds arose from the photolysis of vinyl acetate. It was postulated that as the process continued the double bonds became polyconjugated and responsible for the yellow to brown discoloration. The discoloration phenomenon was considered comparable to that which occurs in PVC on the loss of HCl. In subsequent spectroluminescence investigations it was shown the luminescence of weathered EVA had some characteristics in common with *trans*-β-carotene, a conjugated polyene.[16]

The loss of HCl from PVC on thermal degradation occurs via step-wise elimination from allylic chloride units. Elimination of less than 1.5% of the total HCl content had been found to produce discoloration.[17] Short chains of conjugated unsaturation in thermally degraded PVC absorb in the ultraviolet, but absorption in the visible requires the conjugation of more than eight double bonds.[17,18]

The EVA resin for PV module encapsulants contains 33% vinyl acetate by weight which is about 15% vinyl acetate on a molar basis. That means, on average, that there is one vinyl acetate unit for every six ethylene units (i.e. Et_6VA).

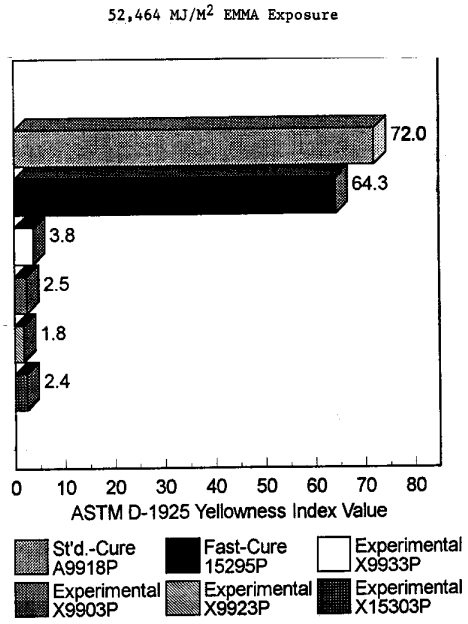

Fig. 7. Yellowness index of experimental encapsulants on exposure in XAW for 30 weeks.

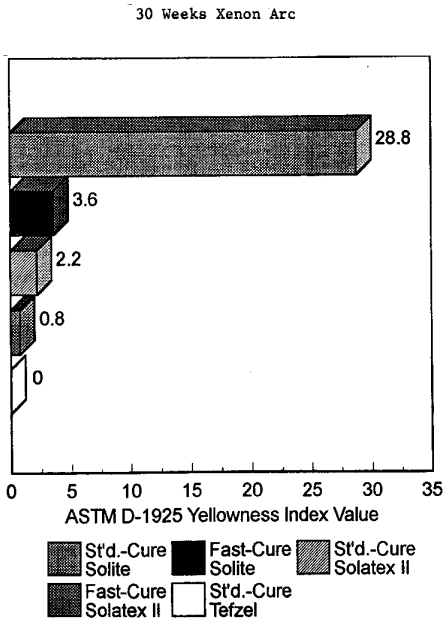

Fig. 8. Yellowness index of various encapsulant/glass superstrate compositions on EMMA exposure for 1 year (52 464 MJ/m^2).

Because of this, and since reactivity ratios for ethylene and vinyl acetate are unity for the high pressure polymerization of EVA,[19] it is not reasonable to expect the formation of long poly(vinyl acetate) segments during polymerization which could give rise, by photolysis, to chains of more than eight conjugated double bonds during weathering of PV modules. Moreover, an investigation of EVA with 40 wt% VA by carbon-13 NMR showed that sequences of three and five VA units were too weak to be observed.[20] Certainly, based on those results, it is not expected that the EVA in PV module encapsulants with 33% VA would be able to generate enough long chains of conjugated double bonds to be a major source of discoloration in field-aged encapsulant.

Several published papers report studies on the photolysis of poly(vinyl acetate) (PVA) and EVA which were carried out using high pressure mercury light sources and irradiation of 253.7 nm. Those studies turn out to be of limited relevance to exposures in terrestrial sunlight whose lowest wavelength is about 290 nm. Product distributions, in mol%, from the photolyses, at 253.7 nm, of EVA (24 mol%, 49 wt% VA), reported by Buchanan and McGill, were 64.9% acetic acid, 26.2% acetaldehyde, 5.2% carbon dioxide and 1.7% ethane, methane and CO, combined.[21] Overall quantum yields were 0.1974 for acetic acid, 0.0795 for acetaldehyde, 0.0159 for carbon dioxide and 0.0113 for combined ethane, methane and CO.[22] The quantum yields for main chain scissioning and cross-linking were 0.0043 and 0.0036, respectively.

In photolysis at 253.7 nm, Norrish I reactions formed free radicals by breaking any one of three single bonds, either C–O, O–C=O or O=C–CH_3 in the acetate functionality. The product yields and quantum yields of the previous paragraph indicate the order of breaking of the single bonds was in the order C–O > O–C=O > O=C–CH_3. The Norrish II reaction would be expected to yield acetic acid and a double bond in the polymer backbone. From the data supplied, it is not possible to distinguish how much acetic acid came from Norrish I and how much came from Norrish II.

Another publication confirmed significant involvement of both Norrish I and Norrish II reactions during photolysis of EVA at 254 nm.[23] However, in that work, apparently the only one reporting results from the photolysis of EVA at terrestrial wavelengths, photolyses of EVA were carried out both at 254 and >300 nm. It was concluded that at 254 nm photo-oxidation is direct but at >300 nm it is indirect and dependent on chromophoric defects, which

follows from the direct generation of free radicals by Norrish I reactions at 254 nm but not at 300 nm. The authors cautioned that attention be paid to the choice of wavelength used in investigations to properly simulate natural weathering.

The TGA results for EVA reported in Section 4.1, the Raman results in 4.5, the infrared results in 4.10 and the results with peracetic acid in 4.7 all question conjugated double bonds as the cause of discoloration of the EVA-based encapsulant in field-aged PV modules. Everything considered, it does not appear likely that the discoloration of EVA-based encapsulant in weathered PV modules is due to long chains of conjugated double bonds as in the case of PVC. Based on published literature articles, the photolysis of EVA at terrestrial wavelengths might be expected to yield double bonds and acetic acid via Norrish II reactions. However, the average length of conjugation would be expected to be considerably less than eight and, therefore, to absorb in the ultraviolet and not in the visible.

5.2 Role of peroxide in discoloration of EVA-based encapsulant

The work with laboratory-prepared laminates has shown that significant amounts of peroxide survived the lamination process and that a few weeks' exposure in the XAW was required to consume it completely (Table 7). During lamination, the peroxide was thermally, homolytically cleaved into alkoxy radicals which abstracted hydrogen atoms from the polymer to cross-link it. During lamination, the alkoxy radicals also have the possibility to react with certain of the stabilizing additives to transform them into precursors of chromophores which develop color on subsequent exposure to sunlight. During exposure to sunlight, any peroxide molecules which survived lamination were photolytically, homolytically cleaved and continued the reactions of alkoxy radicals with the polymer and additives.

Several select laminated formulations were prepared to investigate the influence of peroxide on the ultraviolet absorber and hindered amine. UVA concentrations suffered little reduction when EVA without peroxide was exposed in the XAW for 10 weeks. However, samples with the usual amount of peroxide exhibited a 40% reduction in UVA concentration during 12 weeks exposure (Table 5). That result raises the prospect that interactions between peroxide and UVA under photolysis conditions not only reduce the concentration of an important stabilizing additive but might play a role in color development. In fact, the yellowness index (YI) of the sample without peroxide was 5, that with peroxide was 14 and a sample with twice the usual amount of UVA was 28 after 10–12 weeks of XAW exposures. These results and those in Table 6 suggest the possible involvement of excess peroxide and UVA in discoloration. Scheme 1 depicts some of the initial interactions which are possible between alkoxy radicals from homolysis of peroxide and UVA, which would be expected to give rise to chromophore precursors.

The concentration of HALS behaved similarly, showing slight to no reduction in laminates without peroxide and 61% reduction in laminates with peroxide, after 10–12 weeks' exposure. Changes in concentrations of HALS are mitigated by the fact that its transformation products, nitroxyl and iminoether (Scheme 2), are active stabilizers. Significantly, the samples with HALS did not develop color during exposure in the XAW, including the samples with peroxide.

BHT is infamous for undergoing oxidative transformation into a substituted stilbenequinone, which has one of the highest extinction coefficients for absorption of visible light of any compound associated with polymer stabilizers. As little as 5 ppm in high density polyethylene produced enough color to be discernible.[24] Although Elvax 150 from Dupont contained nominally 400 ppm of BHT, the low levels of

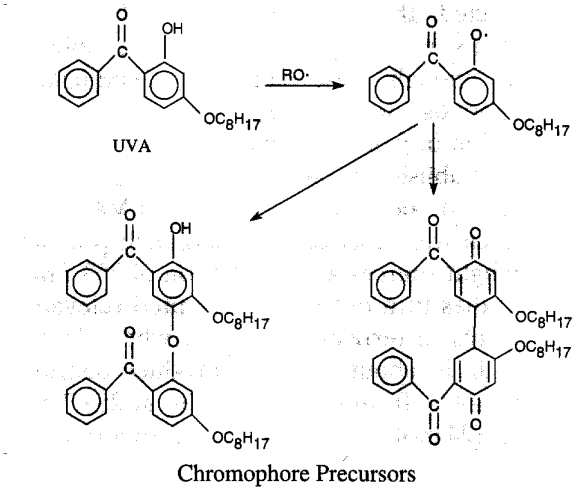

Scheme 1. Transformation of UVA by reaction with peroxide homolysis products.

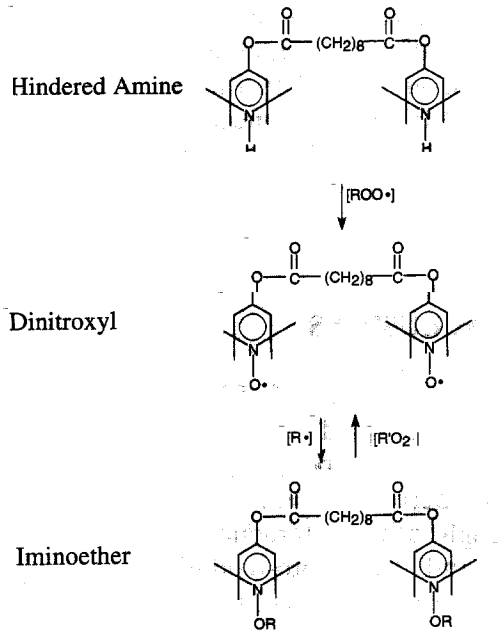

Scheme 2. Transformation of HALS by reaction with oxidation-propagating free radicals.

color in laminates without any additives and in those with peroxide only, exposed in the XAW for up to 15 weeks, suggest that BHT is not involved in the discoloration problem.

It is likely that the phosphite reacted with the peroxide during extrusion and storage of sheets of the encapsulant formulation and was oxidized to the corresponding phosphate. Moreover, the phosphite probably contained small amounts of unreacted nonyl phenol, more of which was likely formed via hydrolysis. Nonyl phenol is expected to be oxidized to colored oxidation products which are typical of phenols. The data for the laminates without phosphite in Table 6 when compared with data for the full formulation, A9918P, suggest the phosphite and peroxide contribute to the discoloration problem.

The experimental results reviewed here reveal significant involvement of the peroxide in the discoloration problem of the encapsulant. Replacement of the peroxide in formulation A9918P with one having a half-life, and at a concentration which would permit it to be consumed completely in the lamination step, is highly desirable. New fast-cure formulations have been developed with a different peroxide which shows promise of much improved color performance.[2]

Since the phosphite and UVA in formulation A9918P are also implicated in the discoloration problem, new experimental formulations have been prepared which take advantage of the findings of this work — problematic additives have been replaced with ones which have provided much superior performance. In addition, new cerium-containing glasses, which absorb more far-UV radiation than glasses which were available before, have also helped reduce encapsulation discoloration considerably. As a result of this work, much progress has been made in improving the performance of the EVA-based encapsulant formulation.[2]

5.3 Significance of colorless areas in discolored panels

Most of the discolored, weathered panels in this investigation contained colorless, diamond-shaped regions where the corners of four silicon cells met (Fig. 2). In addition, the EVA-based encapsulant at the perimeters of the individual silicon cells and at the perimeters of the modules was lighter in color than the EVA encapsulant above the silicon. A few discolored panels contained silicon cells with small cracks, the encapsulant above which was virtually colorless. Micro Fourier transform infrared spectroscopy of these regions of colorless encapsulant showed the presence of absorption bands due to hydrogen-bonded hydroxyl centered at about 3500 cm^{-1}. The IR spectra of the diamond-shaped and cracked areas were qualitatively identical in this region and were similar to the absorption reported for EVA photo-oxidized in air.[23] Discolored regions of EVA-based encapsulant exhibited little, if any, absorption in this region. The hydroxyl group might be present as carboxylic acid, COOH; this would have to be confirmed by further investigation. XPS data provide evidence for ketones in discolored areas but not in the colorless areas.

Hydroxyl absorption in the IR is an indicator that the polymer in those regions underwent oxidation. This suggests that the backing was permeable to oxygen which diffused into the rear of the modules and migrated through regions without the silicon wafer barriers. The clear areas were conduits for oxygen from the back to the front of the modules. These regions with relatively high oxygen exposure might have been 'photo-oxidatively bleached'. Although the possible bleaching of discolored EVA by oxygen might be considered a favorable result, photo-oxidation is not a desirable process to be taking place in organic polymer systems which are

desired to last for 30 years. A desirable objective, for long module life, is to prevent both discoloration and photo-oxidation in PV modules.

The light-colored areas are regions of active additive transport from the lower encapsulant layer, below the silicon cell, to the upper layer above the silicon cell. The two layers are in contact with each other where there is no silicon barrier between them. The depletion of stabilizers and photo-oxidation which took place in the upper part of the cells induced concentration gradients and migration from the rear of the cell through the clear areas. The oxygen which was involved in the migration obviously entered through the backing sheet at the rear of the module.

5.4 XPS results and encapsulant oxidation

The experimental results in Section 4.6 confirm that the encapsulant next to the glass had been extensively oxidized. A reasonable scenario is photo-oxidation involving oxygen which enters the modules through the permeable backing material. This is a highly significant result because it demonstrates clearly that encapsulant was oxidized in the Carrisa Plains modules, and presumably also in other modules of similar construction. The overall ratios of carbon to oxygen in various samples (Table 9) provide a measure of the degree of oxidation: calculated for 33 wt% VA EVA, 8.0; cured, but unaged laboratory-prepared laminate, 7.8; encapsulant next to silicon cell in Carrisa Plains Module #3, 5.5; encapsulant next to top glass in the same module, 4.7; colorless area, 6.5. Although, as expected, the most discolored sample showed the highest degree of oxidation, considerable oxidation was experienced also by the encapsulant next to the silicon in the cell, and in the colorless areas. It should be remembered that, although evidence of oxidation is undisputable, the XPS results are from very thin sections (0.01 μm) and might not be representative of the bulk. More and extensive investigation is required.

Encapsulant oxidation must be minimized in order for PV modules to achieve the longest possible useful life. Oxidation is undesirable, not only because it can cause embrittlement of the encapsulant with reduced protection of the silicon wafers, but also because the discoloration of degraded modules is probably, in part, due to oxidized EVA. All evidence, IR and XPS, indicates that the vinyl acetate moieties have been less affected than the ethylene moieties in degraded EVA. It is conceivable that some of the discoloration was due to severe oxidation of EVA which is similar to severe oxidation of polyethylene.

6 CONCLUSIONS

The discoloration of EVA-based encapsulant samples examined in this investigation is most likely due to peroxide-additive interactions, notably peroxide-UVA and peroxide-phosphite (although other interactions cannot be eliminated) and to photo-oxidation of the EVA. Discoloration due to conjugated double bonds, as in PVC, is deemed not to be a factor. Evidence for metal contamination of the encapsulant in the most discolored regions was not found. However, because copper and silver conductors are used to conduct electricity from the silicon wafers, and because evidence of oxidation was found in the encapsulant above the silicon, metal-catalyzed oxidation might play a role in the degradation. That possibility could be investigated separately.

Efforts should be made to minimize oxidation in PV modules through the use of backing materials which are more impervious to oxygen than currently used materials and by the use of appropriate stabilizers in sufficient amounts to protect the encapsulant for as long as possible, hopefully for the desired 30 years.

More work on the degradation and stabilization of encapsulants in PV modules is needed to assure long-term success of this important renewable energy source. Reformulation to avoid problematic additives and the use of cerium oxide containing glasses have resulted in EVA-based encapsulants which have developed only slight discoloration on exposure to simulated sunlight for long periods of time. These developments should provide much improved performance in future PV modules.

ACKNOWLEDGEMENTS

The authors gratefully acknowledge the following assistance: resonance-enhanced laser Raman investigations of encapsulant samples and PVC carried out by Q. Wu and W. Nelson of the

University of Rhode Island, Kingston, RI 02881. X-ray photoelectron spectroscopic investigations of encapsulant samples carried out by J. Pickering of the Institute of Materials Science, University of Connecticut, Storrs, CT 06268.

This work was made possible by the US Department of Energy through subcontract ZAG-3-11219-02-105661 to Springborn Laboratories, Inc. from the National Renewal Energy Laboratory (NREL), Golden, CO. These studies are part of NREL's on-going Photovoltaic Manufacturing Technology (PVMat) program, under Phase 3A, Shared Process Issues. The Project Coordinator is Holly Thomas of NREL.

REFERENCES

1. Wohlgemuth, J. H. and Petersen, R. C., in *Solar Cells: Their Science, Technology, Application and Economics*. Elsevier Sequoia, 1991, p. 383.
2. Galica, J. P., Holley, W. H., Agro, S. C., Yorgensen, R. S., Ezrin, M., Klemchuk, P. and Lavigne, G., in *Proceedings of 13th European Photovoltaic Conference*, 23–27 October 1995, Nice, France.
3. Springborn Laboratories, Inc. Semi-annual technical progress report on PVMat to national renewable energy laboratory, Subcontract No. ZAG-3-11219-02-105661, 5 November 1993.
4. Pern, F. J. & Czanderna, A. W., *Solar Energy Materials and Solar Cells*, **25** (1991) 3.
5. Petersen, R. C. and Wohlgemuth, J. H., in *Conference Record of the 22nd IEEE Photovoltaic Specialties Conference*, Las Vegas, 1991, p. 562.
6. Schaefer, J., Rosenthal, A., Schlueter, L. and Wenger, H., in *10th European Photovoltaic Solar Energy Conference*, Lisbon, Portugal, April 1991.
7. Garcia, A., III, in *Proceedings of The Flat-Plate Solar Array Project Research Forum on Quantifying Degradation*, 6–8 December 1982, Williamsburg, VA (JPL Publication 83-52).
8. Willis, P. W., Investigation of test methods, material properties and processes for solar cell encapsulants. Final report, Jet Propulsion Laboratory, JPL Contract 95427, August 1986.
9. Rosenthal, A. L. & Lane, C. G., *Solar Cells*, **30** (1991) 563.
10. Krause, A., Lange, A. and Ezrin, M., *Plastics Analysis Guide: Chemical and Instrumental Methods*. Hanser, Munich, 1983, p. 267.
11. Ezrin, M. & Lavigne, G., Failure analysis using gas chromatography/mass spectroscopy, SPE ANTEC Preprints, 2230–2233, Montreal, 1991.
12. Jalbert, C. A., Ph.D. thesis, University of Connecticut, 1993.
13. Atlas Electric Devices Company, Specifications for Atlas Ci35A Xenon WeatherOmeter.
14. Ashley, J. C., *J. Electron Spectrometry*, **28** (1982) 177.
15. Wirsen, A. & Flodin, P., *J. Appl. Polym. Sci.*, **23** (1979) 2005.
16. Pern, F. J., *Polym. Degrad. Stab.*, **41** (1993) 125.
17. Abbas, K. B. & Sorvik, E. M., *J. Appl. Polym. Sci.*, **23** (1975) 2991.
18. Sastre, R., Martinez, G., Castillo, F. & Millan, J. L., *Die Makromol. Chemie, Rapid Commun.*, **5** (1984) 541.
19. Zutty, N. L. and Burkhart, R. D., in *Copolymerization*, ed. G. Ham. Interscience, New York, 1964.
20. Sung, H. N. & Noggle, J. H., *J. Polym. Sci., Polym. Phys. Ed.*, **19** (1981) 1593.
21. Buchanan, K. J. & McGill, W. J., *Polym. J.*, **16** (1980) 309.
22. Buchanan, K. J. & McGill, W. J., *Polym. J.*, **16** (1980) 319.
23. Glickman, J.-F., Arnaud, R. & Lemaire, J., *Makromol. Chem.*, **188** (1987) 989.
24. Klemchuk, P. P. & Horng, P.-Li. *Polym. Degrad. Stab.*, **34** (1991) 333.